Available online at www.sciencedirect.com
SCIENCE DIRECT®
Journal of Photochemistry and Photobiology A: Chemistry 157 (2003) 237–245
Journal of Photochemistry and Photobiology A:Chemistry
www.elsevier.com/locate/jphotochem

Kinetics of the reactions of the hydroxyl radical with CH_3OH and C_2H_5OH between 235 and 360 K

E. Jiménez [a,b,1], M.K. Gilles [a,b,2], A.R. Ravishankara [a,b,*,3]

[a] *Aeronomy Laboratory, NOAA, 325 Broadway, Boulder, CO 80305-3328, USA*
[b] *Cooperative Institute for Research in Environmental Sciences, University of Colorado, Boulder, CO 80309, USA*

Received 23 August 2002; accepted 14 September 2002

Abstract

The kinetics of the reaction of the hydroxyl radical (OH) with methanol (1, rate coefficient k_1) and ethanol (2, rate coefficient k_2), has been studied as a function of temperature (T = 235–360 K and T = 227–360 K, respectively) by using laser photolysis of a suitable OH-precursor to generate OH and laser-induced fluorescence to detect it. The rate coefficients for reactions (1) and (2) are given by the following expressions (in cm^3 $molecule^{-1}$ s^{-1}): $k_1(T) = (3.6 \pm 0.8) \times 10^{-12} \exp(-(415 \pm 70)/T)$ and $k_2(T) = (4.3 \pm 0.7) \times 10^{-12} \exp(-(85 \pm 35)/T)$, respectively, where the uncertainties include the precision of the fit to the Arrhenius expression and estimated systematic errors ($\pm 2\sigma$). Our results are consistent with H-atom abstraction taking place primarily at the methyl site of methanol and at the methylene site for ethanol. The atmospheric implications of these reactions are also discussed.

Keywords: Hydroxyl radical; Methanol; Ethanol; Kinetics; Atmospheric chemistry

1. Introduction

Methanol and ethanol appear to be ubiquitous in the atmosphere. They are released due to the usage as fuels (especially, ethanol), additives to fuels, and in paints, as well as from biomass burning and from damaged plants. Methanol and ethanol are removed from the atmosphere *via* their reaction with hydroxyl radicals, OH. The reaction of OH with alcohols is also a crucial step in their combustion.

$$OH + CH_3OH \rightarrow \text{products} \quad (1)$$

$$OH + C_2H_5OH \rightarrow \text{products} \quad (2)$$

Reaction (1) can proceed by two exothermic channels; the H-atom abstraction from the OH-group or the H-atom abstraction from the methyl group [1,2].

$$OH + CH_3OH \rightarrow H_2O + CH_3O, \quad \Delta H^\circ_{298} = -62.4\,kJ\,mol^{-1} \quad (1a)$$

$$OH + CH_3OH \rightarrow H_2O + CH_2OH \quad \Delta H^\circ_{298} = -99.6\,kJ\,mol^{-1} \quad (1b)$$

The possible exothermic pathways in Reaction (2) are:

$$OH + C_2H_5OH \rightarrow H_2O + C_2H_5O, \quad \Delta H^\circ_{298} = -56.3\,kJ\,mol^{-1} \quad (2a)$$

$$OH + C_2H_5OH \rightarrow H_2O + CH_3CHOH, \quad \Delta H^\circ_{298} = -110\,kJ\,mol^{-1} \quad (2b)$$

$$OH + C_2H_5OH \rightarrow H_2O + CH_2CH_2OH \quad \Delta H^\circ_{298} = -63\,kJ\,mol^{-1} \quad (2c)$$

The enthalpies of these reactions, ΔH°_{298}, are taken from Meier et al. [3].

Previously, k_1 has been measured at 298 K by using absolute techniques [4–6] and relative methods [7–10]. The rate coefficients k_{1a} and k_{1b} have been also calculated using ab initio methods [11]. The kinetic studies of k_2 are less numerous than for k_1, but they have also been measured using both absolute [5,6] and relative methods [7,10,12]. Branching ratios in reactions (1) and (2) have been determined at room temperature by several authors [3,4,11,13,15,16]. According to these studies, it is assumed that H-atom abstraction from the aliphatic chain (Reactions (1b) and (2b)) is the dominant channel at atmospheric temperatures.

* Corresponding author.
E-mail address: ravi@al.noaa.gov (A.R. Ravishankara).
[1] Permanent address: Departamento de Química Física, Facultad de Ciencias Químicas, Universidad de Castilla-La Mancha, Camilo José Cela 10, 13071 Ciudad Real, Spain.
[2] Current address: Ernest Orlando Lawrence Berkeley National Laboratory, 1 Cyclotron Road, Berkeley, CA 94720, USA.
[3] Also associated with the Department of Chemistry and Biochemistry, University of Colorado at Boulder, Boulder, CO 80309, USA.

1010-6030/03/$ – see front matter © 2003 Elsevier Science B.V. All rights reserved.
doi:10.1016/S1010-6030(03)00073-X

Even though the temperature dependence of k_1 and k_2 have been studied at $T > 298$ K, they are not well characterized at tropospheric temperatures [3,11,13–18]. For example, k_1 has been measured only at 260 K by Greenhill and O'Grady [19] and at 240 K by Wallington and Kurylo [20], and k_2 has been measured at 255 and 273 K by Greenhill and O'Grady [19] and at 240 K by Wallington and Kurylo [20]. This lack of data at temperatures relevant to the atmosphere has led to large uncertainties in the recommended values of k_1 and k_2.

In this work, we report the temperature dependence of k_1(235–360 K) and k_2(227–360 K) at temperatures relevant for the atmosphere.

2. Experiments

The apparatus and procedures employed in the current kinetic study have been previously described in detail [21]. The experiments involve excimer laser photolysis of mixtures of an OH precursor, reactant, and He followed by laser-induced fluorescence detection of the OH radical. A jacketed Pyrex reaction cell with an internal volume of *ca.* 200 cm^3 was used in all experiments. The temperature inside the cell was held constant (±1 K) by circulating through a jacket heated ethylene glycol above room temperature and cooled methanol below room temperature.

Photolysis of H_2O_2 ($(0.6 - 4.3) \times 10^{14}$ molecule cm^{-3}) or HNO_3 ($(0.7 - 1.6) \times 10^{15}$ molecule cm^{-3}) at 248 nm was used to generate OH radicals. The photolysis light source was a KrF-excimer laser with fluences in the range of (1.9–6.0) mJ cm^{-2} per pulse in the reactor. The initial OH concentration, $[OH]_0$, was estimated by using the measured fluence (and hence the number of photons cm^{-2} per pulse, N), the absorption cross-section of the precursor at the photolysis wavelength (σ_λ), the quantum yield for OH production from the precursor at this wavelength (ϕ_λ), and concentration of the precursor ([precursor]):

$$[OH]_0 = N\sigma_\lambda\phi_\lambda[\text{precursor}] \quad (3)$$

The quantum yield for OH in H_2O_2 and HNO_3 at 248 nm were taken to be 2 and 1, respectively [2]. The calculated $[OH]_0$ ranged from 3.6×10^{10} molecule cm^{-3} to 4.2×10^{11} molecule cm^{-3}. OH radicals were excited in the $A^2\Sigma^+ \leftarrow X^2\Pi$ vibronic band (282 nm) by using the doubled output of a pulsed dye laser pumped by a Nd:YAG laser. The laser-induced fluorescence was imaged onto the photocathode of a photomultiplier tube (PMT) after passing through a bandpass filter (peak transmission at 310 nm with a bandpass of ±10 nm, FWHM). The PMT signal was averaged with a gated charge integrator and recorded by a computer.

In most experiments, alcohol concentrations were determined from gas flow rates measured using calibrated mass flow meters and the total pressure inside the reaction cell. In some experiments at 298 and 259 K, methanol concentrations were determined both before entering and after leaving the reaction cell by UV absorption at 185 nm (using a pen-ray Hg lamp and a 50-cm length cell held at 298 K). The methanol absorption cross section at 185 nm was measured to be $(6.3 \pm 0.1) \times 10^{-19}$ cm^2 $molecule^{-1}$, in good agreement with the literature value [22]. The methanol concentrations in the reaction cell were calculated from the measured concentrations in the absorption cells after accounting for the temperatures and pressures in the reactor and absorption cells. Reactant concentrations ranged from $(0.9 - 23) \times 10^{15}$ molecule cm^{-3} for CH_3OH and $(0.3 - 3.9) \times 10^{15}$ molecule cm^{-3} for C_2H_5OH. The gas mixture containing the alcohol, the OH photolytic precursor, and the bath gas at a total pressure of 26–51 Torr was flowed through the cell at a linear flow velocity of 7–22 cm s^{-1}. Since the laser repetition rate was 10 Hz, the gas mixture within the detection volume, defined as the volume produced by the photolysis beam that could be interrogated by the probe laser beam, was replenished between laser pulses.

2.1. Chemicals

Helium buffer gas (99.999%) was used without purification. Methanol (Fisher Scientific, 99.9 %) and ethanol (Sigma–Aldrich, >99.5 %) were degassed by repeated freeze-pump-thaw cycles. Hydrogen peroxide, H_2O_2, was concentrated (>90%) by bubbling a small flow of He through a 60% solution prior to use. Nitric acid was synthesized by the reaction of sulfuric acid with $NaNO_3$ and collected in a glass bubbler. This bubbler was kept in a salt/ice bath at 260 K to decrease HNO_3 vapor pressure and, hence, make it easier to control the nitric acid concentration in the reaction cell.

3. Results and discussion

All experiments were carried out under pseudo-first order conditions in OH ([ROH] > 1000$[OH]_0$; [ROH] is the methanol or ethanol concentration). Under these conditions, the OH temporal profiles followed the pseudo-first order rate law given by:

$$\ln[OH]_t = \ln[OH]_0 - k_i' t \quad (4)$$

where,

$$k_i' = k_i[\text{ROH}] + k_0' \quad (5)$$

k_i' is the measured pseudo-first order decay rate coefficient and k_i is the second-order rate coefficient for the reaction of OH with methanol ($i = 1$) or ethanol ($i = 2$). k_0' is the pseudo-first order rate coefficient obtained in the absence of the alcohol and is essentially the sum of the first-order rate coefficients for the reaction of OH radical with its photochemical precursor and impurities, and the OH diffusion out of the detection zone ($k_0' = (80 - 660)$ s^{-1}). The values of

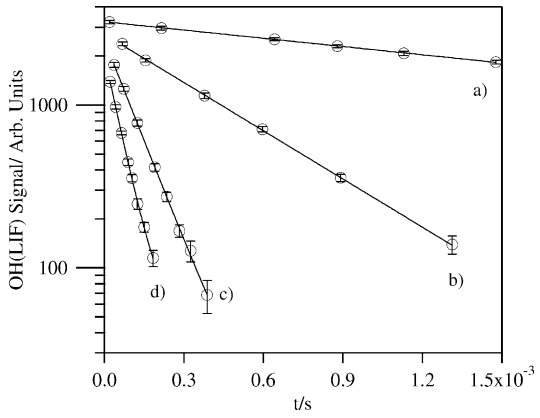

Fig. 1. OH temporal profiles registered in the photolysis of several H_2O_2/CH_3OH/He mixtures at $T = 244$ K, in varying concentrations of CH_3OH (a) 0; (b) 0.26; (c) 1.34 and (d) 2.32 (in $\times 10^{16}$ molecule cm^{-3}).

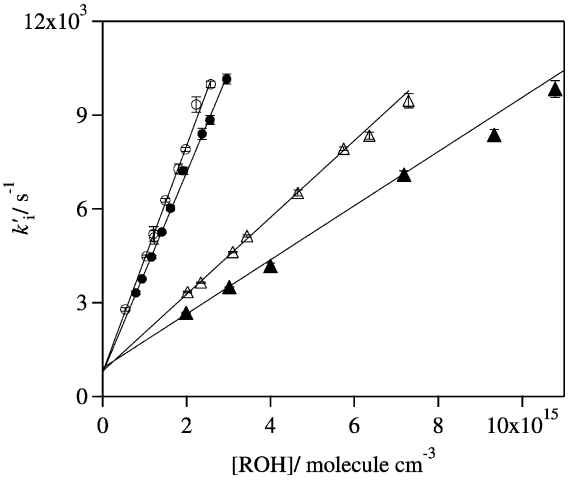

Fig. 2. Pseudo-first order rate coefficient, k'_i, vs. alcohol concentration at two temperatures: $T = 285$ K for methanol (▲) and ethanol (●) and $T = 360$ K for methanol (△) and ethanol (○).

k'_i were extracted from the linear least-squares analysis of Eq. (4). Some examples of the measured temporal profiles of OH at 244 K in the presence of various concentrations of CH_3OH are shown in Fig. 1. In all cases, the measured OH profiles were exponential, confirming that the loss rates of OH were pseudo-first order in [OH].

Tables 1 and 2 list the measured values of k_1 and k_2, and the experimental conditions employed. At each temperature, k_1(T) and k_2(T) were obtained from the slopes of the plots of k'_1 and k'_2 against the concentration of the alcohol *via* linear least-squares analyses. The quoted uncertainties of the rate coefficients $k_1(T)$ and $k_2(T)$ include only the precision ($\pm 2\sigma$) of the fit of k'_i versus [ROH] data to Eq. (5). Fig. 2 shows such plots for the reactions of OH with methanol and ethanol at 285 and 360 K.

Our measured values of k_1 and k_2 were not affected by changes in the residence time of the gas mixture in the reaction cell, fluence of the photolysis laser or total pressure. Two different OH precursors (H_2O_2 and HNO_3) were used at $T > 298$ K and the initial OH concentration was varied

Table 1
Summary of the rate coefficient for the OH + CH_3OH reaction and the experimental conditions employed in the present study

T (K)	p (Torr)	[Precursor] $\times 10^{-14}$ (molecule cm^{-3})	$E_{\lambda=248\,nm}$ (mJ cm^{-2} per pulse)	$[OH]_0 \times 10^{-11}$ (molecule cm^{-3})	v (cm s^{-1})	$[CH_3OH] \times 10^{-15}$ (molecule cm^{-3})	k'_1 (s^{-1})	$(k_1(T) \pm 2\sigma)$[a] $\times 10^{13}$ (cm^3 molecule^{-1} s^{-1})
235	50	0.7	4	0.5	7	4.4–18	2562–10709	6.22 ± 0.93
235	51	6.9[b]	3	0.4	8	2.6–23	826–3087	6.43 ± 1.23
244	36	2.4	5	2.1	9	2.6–23	2273–16232	6.73 ± 0.05
251	36	2.1	3	1.1	9	1.0–13	1059–15848	7.29 ± 0.33
259	35	2.6	3	1.5	11	1.7–14	1649–12762	7.11 ± 0.42
259	32	3.7	6	4.2	8	2.2–22[c]	5543–16558	6.85 ± 0.59
261	41	14[b]	3	0.9	9	2.9–13	831–10555	6.70 ± 0.49
273	35	3.1	4	2.4	10	2.1–15	2300–11830	7.67 ± 0.17
273	34	4.3	4	2.8	10	1.0–13	2824–15634	7.51 ± 0.10
285	37	3.8	3	2.1	11	2.0–18	2676–16489	8.66 ± 0.36
298	26	1.9	5	1.5	22	0.9–12[c]	1451–11912	9.12 ± 0.39
298	26	2.5	5	2.0	22	1.6–11[c]	2163–10863	9.18 ± 0.52
298	31	2.6	6	3.0	9	2.4–12[c]	2073–10930	8.14 ± 1.13
298	50	0.6	4	0.4	9	2.7–14	2776–12232	8.45 ± 0.70
298	36	3.4	3	2.1	11	0.9–14	1597–13838	9.47 ± 0.17
298	43	16[b]	3	1.1	9	3.9–14	3883–13186	8.69 ± 0.72
315	36	2.9	3	1.6	12	2.2–11	2811–11712	9.53 ± 0.14
330	35	2.8	3	1.5	12	1.7–12	2565–13722	10.3 ± 0.27
345	38	2.9	3	1.6	13	1.7–12	2847–12285	11.3 ± 0.54
360	36	2.3	3	1.4	13	1.4–8.8	3375–12620	13.5 ± 0.62
360	36	2.0	3	1.0	11	2.0–8.8	3339–10589	12.3 ± 0.46

The bath gas was He.

[a] Uncertainties in $k_1(T)$ represent only the precision of the fit.

[b] OH precursor was HNO_3 instead of H_2O_2.

[c] Methanol concentrations were determined by UV absorption measurements.

Table 2
Summary of the rate coefficient for the OH + C_2H_5OH reaction obtained and the experimental conditions employed in the present study

T (K)	p_T (Torr)	[Precursor] × 10^{-14} (molecule cm^{-3})	$E_{\lambda=248\,nm}$ (mJ cm^{-2} per pulse)	$[OH]_0$ × 10^{-11} (molecule cm^{-3})	v (cm s^{-1})	$[C_2H_5OH]$ × 10^{-15} (molecule cm^{-3})	k'_2 (s^{-1})	($k_2(T) \pm 2\sigma$)[a] × 10^{12} (cm^3 $molecule^{-1}$ s^{-1})
227	40	0.9	3.2	0.5	7	0.5–3.0	2519–10300	2.80 ± 0.23
243	41	1.4	4.1	1.0	8	0.7–3.8	2577–11771	3.11 ± 0.10
260	41	1.7	3.6	1.1	8	0.5–2.9	2201–9798	3.20 ± 0.11
273	41	2.3	3.6	1.5	9	0.4–2.7	1937–8944	3.24 ± 0.08
285	41	2.6	3.8	1.8	9	0.8–3.8	3314–10156	3.20 ± 0.10
298	40	13[b]	1.9	0.5	9	0.4–2.4	2174–8747	3.15 ± 0.24
298	40	8.4[b]	2.5	0.4	9	0.9–3.9	3654–13028	3.07 ± 0.12
298	40	7.7[b]	0.5	0.4	9	1.1–3.4	4098–10892	2.99 ± 0.15
300	41	2.4	3.7	1.6	9	0.7–2.6	3293–9310	3.15 ± 0.04
315	41	2.5	3.2	1.5	9	0.4–3.2	3987–10702	3.27 ± 0.10
330	41	3.0	3.2	1.7	9	0.5–2.5	2495–9287	3.00 ± 0.11
330	41	2.2	3.8	1.5	10	0.5–2.8	2443–9899	3.39 ± 0.06
345	40	2.3	3.3	1.4	11	0.5–2.7	2500–10460	3.37 ± 0.22
360	40	2.1	3.5	1.3	11	0.5–2.6	2785–9987	3.60 ± 0.11

The bath gas was He.
[a] OH precursor is HNO_3 instead of H_2O_2.
[b] Uncertainties in $k_2(T)$ represent only the precision of the fit.

by a factor of seven for methanol and a factor of four for ethanol (see Tables 1 and 2). None of these changes influenced the measured rate coefficients. These tests indicate a negligible contribution of secondary chemistry involving OH, its precursor, or photolytic products of the precursor and alcohols, and lend confidence to our measured values. When HNO_3 was used as a precursor of OH radical below 298 K, the OH temporal profiles were not exponential. We do not have a good idea as to what caused such temporal profiles. We suspect that ethanol reacted with HNO_3 on the walls, which led to this behavior. In any case, k_2 was measured below 298 K by photolyzing only H_2O_2.

The estimated systematic uncertainties are ($\pm 2\sigma$): ±2% in total pressure, ±2% in flow rate, and less than 1% in temperature. The uncertainties in the alcohol concentration in the stock mixture and the UV absorption cross-section of methanol also contribute to the systematic errors. Thus, the overall uncertainty in the concentrations of the alcohols in the reaction cell is estimated to be ±5% at the 95% confidence level.

A summary of the results obtained in this work is presented in Tables 3 and 4. The weighted, according to the precision of the measurement ($w_i = 1/\sigma_i^2$), average of the rate coefficients at 298 K is $k_1(298\,K) = (9.3 \pm 1.1) \times 10^{-13}\,cm^3\,molecule^{-1}\,s^{-1}$ for the reaction of OH with methanol and $k_2(298\,K) = (3.1 \pm 0.4) \times 10^{-12}\,cm^3\,molecule^{-1}\,s^{-1}$ for the OH + ethanol reaction; the quoted errors are $\pm 2\sigma$. The uncertainties include the estimated systematic errors cited above. Tables 3 and 4 also list the results from the previous studies and the NASA/JPL [2] and IUPAC [23] recommendations (all errors quoted by the authors). Our value of $k_1(298\,K)$ is in good agreement with most of the previous studies reported in the literature, within their quoted uncertainty limits [4–8,12,15,19,20]. Also our $k_1(298\,K)$ is in excellent agreement with the rate coefficient recommended by the NASA/JPL evaluations [2] and the IUPAC recommendations [23]. The recommended value is the average of seven direct studies ($k_1(298\,K) = 8.9 \times 10^{-13}\,cm^3\,molecule^{-1}\,s^{-1}$) [5,6,13–15,19,20]. The rate coefficient $k_1(298\,K)$ reported by Klöpffer et al. [9] is higher than that reported in this work, possibly due to the indirect method used. On the other hand, the rate coefficient $k_1(298\,K)$ measured by Hägele et al. [13] and by Meier et al. [14,16] is lower than our reported value. The room temperature rate coefficient, $k_2(298\,K)$, from this work is in good agreement with most previous studies [5–7,10–12,17,18] and with the recommended value, $k_2(298\,K) = 3.2 \times 10^{-12}\,cm^3\,molecule^{-1}\,s^{-1}$ [2]. It is worth noting that the room temperature values of k_1 and k_2 reported by Meier et al. are lower than those from all the recent studies.

The Arrhenius plots of $k_1(T)$ and $k_2(T)$ measured in this work are presented in Figs. 3 and 4, respectively. The Arrhenius parameters (A and E_a/R) were obtained by weighted linear least-squares analysis of $\ln(k_1)$ and $\ln(k_2)$ versus $1/T$. The obtained temperature dependence expressions of k_1 and k_2 (in $cm^3\,molecule^{-1}\,s^{-1}$) are:

$$k_1(T) = (3.6 \pm 0.8) \times 10^{-12} \exp(-(413 \pm 70)/T)$$

$$k_2(T) = (4.3 \pm 0.7) \times 10^{-12} \exp(-(85 \pm 35)/T)$$

where the uncertainties in A and in E_a/R are twice the standard deviation of the fits at the 95% confidence limit ($\sigma_A = A\sigma_{\ln A}$ and σ_{E_a}) plus the contribution of the estimated systematic uncertainties noted earlier. The rate coefficients $k_1(298\,K)$ and $k_2(298\,K)$ extracted from the Arrhenius expressions ($(9.0 \pm 1.5) \times 10^{-13}\,cm^3\,molecule^{-1}\,s^{-1}$ for Reaction (1) and $(3.2 \pm 0.6) \times 10^{-12}\,cm^3\,molecule^{-1}\,s^{-1}$ for Reaction (2)) are in excellent agreement with those measured at that temperature, indicating that the kinetics of these reactions are well described by the corresponding Arrhenius expression.

Table 3
Comparison of the rate coefficient for the OH + CH_3OH reaction obtained in this work with literature values

T (K)	p_T (Torr)	$k_1(298\,K) \times 10^{13}$ (cm^3 $molecule^{-1}$ s^{-1})	$A \times 10^{12}$ (cm^3 $molecule^{-1}$ s^{-1})	E_a/R (K)	Techniques	References
235–360	26–51	9.3 ± 1.1	3.6 ± 0.8	415 ± 70	LP/LIF[a]	This work
298	3	10.1 ± 1.0	–	–	DF/LIF[b]	[4]
296 ± 2	150	10.6 ± 1.0	–	–	FP/RA[c]	[5]
298	20–200	10.0 ± 1.0	–	–	FP/RF[d]	[6]
292	760	9.5 ± 1.0	–	–	Relative method	[7]
300 ± 3	735	10.8 ± 0.8	–	–	Relative method	[8]
300	760	12	–	–	Relative method[e]	[9]
298	760	9.0 ± 0.8	–	–	Relative method	[10]
300–3000	–	7.6	–	–	*Ab initio*	[11]
295–420	10	7.8 ± 1.5	12.0 ± 3.0	810 ± 50	LP/RF[f]	[13]
300–1020	0.6–1.8	7.7	11.0 ± 3.0	798 ± 45	DF/LIF & MS[e,g]	[14,16]
293–866	700	9.43	[h]	[h]	LP/LIF	[15]
260–803	100	8.6	8.0 ± 1.9	664 ± 88	FP/RA	[19]
240–440	25–50	8.61 ± 0.47	4.8 ± 1.2	480 ± 70	FP/RF	[20]
		8.9	6.7	600 ± 300	JPL	[2]
240–300		9.3 ± 1.4	3.1	360 ± 200	IUPAC	[23]

The uncertainties in our k_1, A and E_a/R are $\pm 2\sigma$, and include estimated systematic uncertainties. Uncertainties in the literature values are those quoted by the authors.

[a] Laser photolysis/laser-induced fluorescence.
[b] Discharge flow/laser-induced fluorescence.
[c] Flash photolysis/resonance absorption.
[d] Flash photolysis/resonance fluorescence.
[e] Uncertainties not stated by the authors.
[f] Laser photolysis/resonance fluorescence.
[g] Discharge flow/laser-induced fluorescence or discharge flow/mass spectrometry.
[h] $k_1(T) = (5.89 \pm 0.07) \times 10^{-20}\ T^{2.65} \exp(+444.4/T)$.

The temperature dependences for k_1 and k_2 reported in this work are compared with those from the literature in Figs. 3 and 4, respectively. In these figures, the previous measurements carried out at only room temperature are not included for clarity. Previous determinations of the Arrhenius parameters for k_1 and k_2 show significant scatter in the values of A and E_a/R (see Tables 3 and 4). Only two kinetic studies of reactions (1) and (2) have been performed below room temperature, and even those were at just a few temperatures [19,20]. Thus, the temperature dependence for both rate coefficients below 298 K was not well established. Our data below 298 K help in defining k_1 and k_2 for atmospheric purposes. The uncertainty of k_1 and k_2 at a given temperature (T) is

Table 4
Comparison of the temperature dependence of the rate coefficient for the OH + C_2H_5OH reaction obtained in this work with literature values

T (K)	p_T (Torr)	$k_2(298\,K) \times 10^{12}$ (cm^3 $molecule^{-1}$ s^{-1})	$A \times 10^{12}$ (cm^3 $molecule^{-1}$ s^{-1})	E_a/R (K)	Techniques	References
227–360	40	3.1 ± 0.4	4.3 ± 0.7	85 ± 32	LP/LIF[a]	This work
296 ± 2	150	3.74 ± 0.36	–	–	FP/RA[b]	[5]
298	20–200	2.62 ± 0.36	–	–	FP/RF[c]	[6]
292		3.0 ± 0.3	–	–	Relative method	[7]
298 ± 4	760	3.88 ± 0.11	–	–	Relative method	[10]
295	760	3.1 ± 0.5	–	–	Relative method	[12]
300–1000	1	1.76	4.4 ± 1.0	274 ± 90	DF/LIF & MS[d,e]	[3,16]
300–1000	1	2.06	5.16 ± 1.0	274 ± 90	DF/LIF[d,e]	[17]
293–750	700	3.26 ± 0.14	–	–	LP/LIF[a]	[18]
255–459	100	3.70	12.5 ± 2.4	360 ± 52	FP/RA[b,d]	[19]
240–440	25–50	3.33 ± 0.23	7.4 ± 3.2	240 ± 110	FP/RF[c]	[20]
		3.2	7.0	235 ± 100	JPL	[2]
270–340		3.2 ± 0.5	4.1	70 ± 200	IUPAC	[23]

The uncertainties in our k_2, A and E_a/R are $\pm 2\sigma$ and include estimated systematic uncertainties. Uncertainties in the literature values are those quoted by the authors.

[a] Laser photolysis/laser-induced fluorescence.
[b] Laser photolysis/resonance absorption.
[c] Laser photolysis/resonance fluorescence.
[d] Uncertainties not stated by the authors.
[e] Discharge flow/laser-induced fluorescence or discharge flow/mass spectrometry.

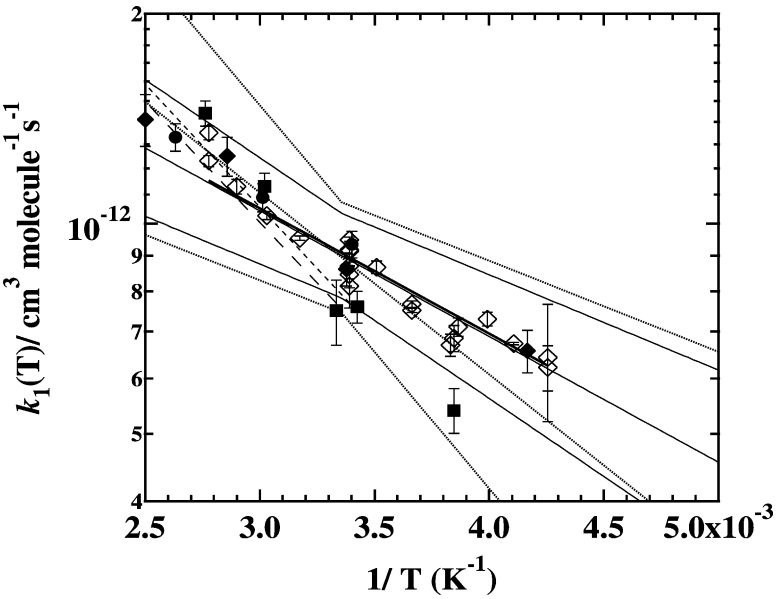

Fig. 3. Arrhenius representation for k_1 obtained in this work (T = 235–360 K) and those of literature data. (◇) Experimental data (this work); (⎯) fit of our data to the Arrhenius expression; (—) our recommendation and error limits; (. . .) JPL recommendation and error limits [2]; (- - -) Hägele et al. [13]; (- - -) Meier et al. [16]; (●) Hess and Tully [18]; (■) Greenhill and O'Grady [19]and (◆) Wallington and Kurylo [20].

expressed, according to the format used in the NASA/JPL evaluations, in terms of f(298 K) and $\Delta E_a/R$ [2]. The previous recommendation for the uncertainty in the room temperature rate coefficient k_1(298 K) was f(298 K) = 1.2. The recommended value E_a/R = (600 ± 300) K for k_1 was based upon the studies of Greenhill and O'Grady [19] and Wallington and Kurylo [20] in the temperature range of 240–400 K. In the case of Reaction (2), the previous recommendation of f(298 K) was 1.3 and the E_a/R value was (235 ± 100) K based on the data of Hess and Tully [18] and Wallington and Kurylo [20].

The temperature dependence for $k_1(T)$ and $k_2(T)$ and the upper and lower uncertainty limits previously recommended by the NASA/JPL evaluations are represented by dotted lines (cited as JPL recommendation and error limits) in Figs. 3 and 4, respectively [2].The uncertainty limits for Reaction (2) are larger, even at room temperature, than those for Reaction (1) because of the scatter in previous data. By

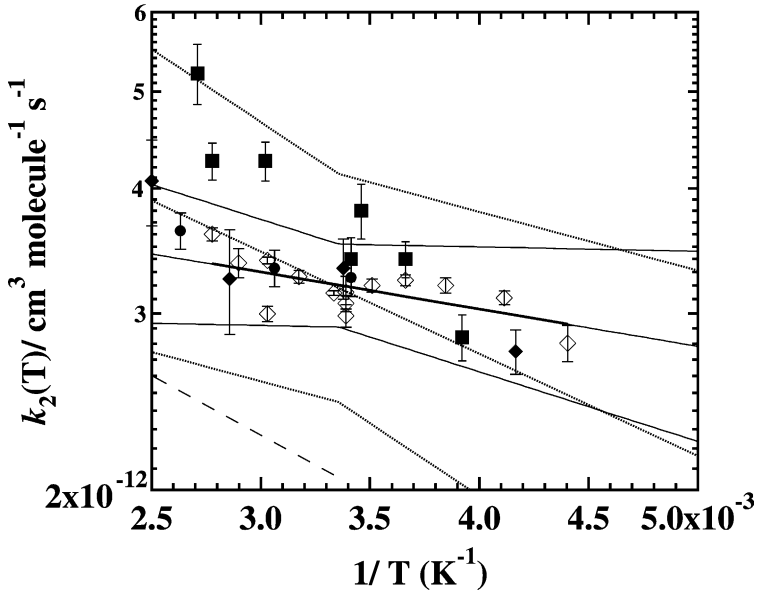

Fig. 4. Arrhenius representation for k_2 obtained in this work (T = 227–360 K) and those of literature data. (◇) Experimental data (this work); (⎯) fit of our data to the Arrhenius expression; (—) our recommendation and error limits; (. . .) JPL recommendation and error limits [2]; (- - -) Meier et al. [17]; (●) Hess and Tully [18]; (■) Greenhill and O'Grady [19]; (◆) Wallington and Kurylo [20].

combining our extensive measurements with previous data, we recommend:

$$k_1(298\,\mathrm{K}) = 9.0 \times 10^{-13}\,\mathrm{cm^3\,molecule^{-1}\,s^{-1}},$$
$$\text{with } f(298\,\mathrm{K}) = 1.15$$

and,

$$k_2(298\,\mathrm{K}) = 3.2 \times 10^{-12}\,\mathrm{cm^3\,molecule^{-1}\,s^{-1}},$$
$$\text{with } f(298\,\mathrm{K}) = 1.1$$

We recommend $A = 3.6 \times 10^{-12}\,\mathrm{cm^3\,molecule^{-1}\,s^{-1}}$, $E_a/R = 415\,\mathrm{K}$ and $\Delta E_a/R$ of 100 K for Reaction (1) and $A = 4.3 \times 10^{-12}\,\mathrm{cm^3\,molecule^{-1}\,s^{-1}}$, $E_a/R = 85\,\mathrm{K}$ and $\Delta E_a/R$ of 75 K for Reaction (2). Our recommended temperature dependence of $k_1(T)$ and $k_2(T)$ and their upper and lower uncertainty limits are represented by a solid line in Figs. 3 and 4, respectively (cited as Our recommendation and error limits). These values of A and E_a/R can be used to calculate k_1 and k_2 at any temperature between 200 and 350 K. The uncertainties in the rate coefficients, $f(T)$, can be calculated using the expression:

$$f(\mathrm{T}) = f(298)\exp\left|\frac{\Delta E_a}{R}\left(\frac{1}{T} - \frac{1}{298}\right)\right| \quad (6)$$

As in previous recommendations, the data from Hägele et al. [13] and Meier et al. [14,16] were not used in deriving the above recommendation, since their studies were restricted to temperatures greater than 298 K. As can be seen in Figs. 3 and 4, the data from Greenhill and O'Grady [19] are outside the range of all previous measurements and, hence, were excluded. Our results better define the behavior of k_1 and k_2 under atmospheric temperatures and greatly decrease the uncertainties in $k_1(T)$ and $k_2(T)$.

Recently, Jodkowski et al. [11] calculated the rate coefficients for the reaction channels (1a) and (1b) at temperatures between 300 and 3000 K using ab initio methods and suggested that k_1 should follow a three-parameter expression of the type $AT^n \exp(-E_a/RT)$, similar to that used by Hess and Tully [15]. The Arrhenius plots observed by Hess and Tully for k_1(293–866 K) [15], showed a strong curvature in the studied temperature range and, hence, they used a three parameter expression, $k_1(T) = (5.89 \pm 0.07) \times 10^{-20}\,T^{2.65} \exp(444/T)\,\mathrm{cm^3\,molecule^{-1}\,s^{-1}}$. However, over the narrow temperature range (235–360 K) studied in our work, the Arrhenius plot for k_1 does not show significant curvature. The lack of curvature is not surprising since the reaction almost exclusively proceeds *via* H-abstraction for the CH_3 group over the small atmospheric temperature range studied here.

Rate coefficients for the reaction of OH with CH_3OH and OH with CD_3OH have been measured by at least three different groups, McCaulley et al. [4], Hess and Tully [15], and Greenhill and O'Grady [19]. McCaulley et al. [4] studied the kinetics of OH and OD radicals with CH_3OH and several deuterated methanols (CH_3OD, CD_3OH and CD_3OD) at 298 K. They observed that deuteration of the hydroxyl group had little effect on the measured rate coefficient. In contrast, the deuterium substitution in the methyl group greatly suppressed the rate coefficients, confirming the dominance of H-abstraction from the methyl group in CH_3OH. Such an isotope effect was also observed by Hess and Tully [15]and by Greenhill and O'Grady [19] in OH reactions with CD_3OH and CH_3OH. Greenhill and O'Grady measured the rate coefficients for the OH reaction with methanol-d_3 at 293 K, while Hess and Tully [15] measured the temperature dependence between 293 and 866 K. Hess and Tully [15] observed that the ratio of the rate coefficients for OH with CH_3OH to that of OH with CD_3OH decreased sharply above 625 K and attributed it to an increase in the relative importance of abstraction from the hydroxyl site at higher temperatures.

Yields of CH_3O from Reaction (1a) have been measured by several groups [3,13,14] to be from 0.11 to 0.25 at room temperature, consistent with the measured yield for CH_2OH at 298 K, (0.75 ± 0.08), by Meier et al. [16]. Thus, the main pathway (about 75%) for the reaction of OH with methanol at room temperature is the abstraction of a hydrogen atom from the CH_3 group. The methoxy radical yield has been observed to increase with increasing temperature [13] and ab initio calculations indicate that at high temperature (>1500 K) more than 90% of the reaction proceeds *via* abstraction of hydrogen from the hydroxyl group [11]. Thus, the linear Arrhenius behavior we observe over the atmospheric temperature range is to be expected.

Hess and Tully [18] also observed a non-Arrhenius behavior for the reaction between the hydroxyl radical and ethanol between 294 and 750 K. These authors observed a decrease in the measured rate coefficients for OH loss between 520 and 600 K, whilst at temperatures lower than 520 K and higher than 600 K the rate coefficients presented a positive temperature dependence. They attributed the decrease of k_2 between 520 and 600 K to the thermal decomposition of CH_2CH_2OH, produced by H abstraction from the CH_3 group (Reaction (2c)), which regenerated OH (and C_2H_4). In the present study of the OH + ethanol reaction, no curvature in the Arrhenius plot for k_2 was observed, confirming that one channel is dominant between 227 and 360 K.

The α-radical, CH_3CHOH, was detected and quantified, (0.75 ± 0.15), at room temperature by Meier et al. [3,16]. Thus, the main pathway for the reaction of OH radical with C_2H_5OH at room temperature seems to be the H-abstraction from the methylene group (Reaction (2b)). In the troposphere, the reaction of OH with ethanol produces mostly CH_3CHOH.

Typical methods for calculating specific site reactivity (i.e. those of Atkinson [24]) display a stronger temperature dependence for abstraction from a methyl group versus a methylene group. Presumably this is due to the greater stability of the more highly substituted radical product of a methylene group. The activation energy obtained in this work for k_1 ($E_a = 3.5\,\mathrm{kJ\,molecule^{-1}}$) is higher than that for k_2 ($E_a = 0.7\,\mathrm{kJ\,molecule^{-1}}$). This observation is consistent with H-atom abstraction occurring primarily at

the methyl site of methanol and at the methylene site for ethanol.

3.1. Atmospheric implications

As mentioned in the Introduction, methanol and ethanol are released into the atmosphere by vehicles, biomass burning, etc. Because they do not significantly absorb in the actinic window of $\lambda > 320$ nm, photolysis of these compounds is much slower than their reaction with OH (Reactions 1 and 2). Using the rate coefficients measured here, one can better define the lifetimes of CH_3OH and C_2H_5OH. The lifetimes of methanol in the presence of 1×10^6 cm^{-3} of OH ($\tau_{CH_3OH} = 1/k_1[OH]$) are about 2 weeks at 298 K and ca. 18 days at 227 K. Under similar conditions, ethanol would have a lifetime of ca. 4 days. Clearly, methanol is longer lived than ethanol and is more likely to reach the upper troposphere.

The product of Reaction (1) under tropospheric conditions, CH_2OH, leads to HO_2 and HCHO in the troposphere. Formaldehyde also leads to the production of HO_2 *via* the sequence of reactions:

$$HCHO + h\nu\ (\lambda < 360\,nm) \rightarrow HCO + H \quad (7)$$

$$HCO + O_2 \rightarrow CO + HO_2 \quad (8)$$

$$H + O_2 + M \rightarrow HO_2 + M \quad (9)$$

Even though a fraction of HCHO photolyzes to give $H_2 + CO$ and a fraction of it reacts with OH, the net reaction of CH_3OH degradation in the troposphere is to produce HO_x (HO_2 and OH). Note that the formation of CH_3O would also lead to HO_2 and HCHO in the atmosphere, just as CH_2OH does.

The main channel for the $OH + C_2H_5OH$ reaction (75% at room temperature [3,16]) seems to be the formation of the α-radical, CH_3CHOH, which can lead to acetaldehyde (CH_3CHO) and HO_2 in the presence of O_2. Photolysis of acetaldehyde in the atmosphere leads partly to HCO and CH_3CO radicals.

$$CH_3CHO + h\nu \rightarrow HCO + CH_3 \quad (10a)$$

$$\rightarrow CH_3CO + H \quad (10b)$$

The reaction of HCO with O_2 produces HO_2 (Reaction (8)) and methyl radical in the presence of oxygen produces methylperoxyl radicals, CH_3O_2:

$$CH_3 + O_2 + M \rightarrow CH_3O_2 + M \quad (11)$$

On the other hand, CH_3CO radicals formed in the photolysis of acetaldehyde (Reaction (10b)) or by reaction with OH,

$$CH_3CHO + OH \rightarrow CH_3CO + H_2O \quad (12)$$

can form peroxyacetyl radical and peroxyacetyl nitrate (PAN) *via* reactions:

$$CH_3CO + O_2 \rightarrow CH_3C(O)O_2 \quad (13)$$

$$CH_3C(O)O_2 + NO_2 \leftrightarrow CH_3C(O)OONO_2(PAN) \quad (14)$$

Thus, the reaction of OH with C_2H_5OH will also contribute to PAN formation in polluted environments and due to the reasonably long lifetime of PAN, particularly at colder temperatures, makes it an important agent for transporting NO_x on regional and global scales. If the H atom of the CH_3 group is removed, the fate of the produced CH_2CH_2OH radical in the atmosphere is expected to be the formation of 2 HCHO and HO_2, and thus to more HO_x. The abstraction of H from the alcohol group should lead to the same products as that from H removal from the methylene group.

Acknowledgements

This work was funded in part by the NASA Upper Atmospheric Research Program. E. Jiménez acknowledges a fellowship from the University of Castilla-La Mancha (Spain).

References

[1] W. Tsang, Chemical kinetic data base for combustion chemistry. Part 2. Methanol, J. Phys. Chem. Ref. Data 16 (1987) 507.
[2] W.B. DeMore, S.P. Sander, D.M. Golden, R.F. Hampson, M.J. Kurylo, C.J. Howard, A.R. Ravishankara, C.E. Kolb, M.J. Molina, Chemical kinetics and photochemical data for use in stratospheric modeling, Evaluation Number 12. JPL Publication 97-4, Jet Propulsion Laboratory, California Institute of Technology, Pasadena, CA, 1997.
[3] U. Meier, H.H. Grotheer, G. Riekert, T. Just, Temperature dependence and branching ratio of the $C_2H_5OH + OH$ reaction, Chem. Phys. Lett. 115 (1985) 221–225.
[4] J.A. McCaulley, N. Kelly, M.F. Golde, F. Kaufman, Kinetic studies of the reactions of F and OH with CH_3OH, J. Phys. Chem. 93 (1989) 1014–1018.
[5] R. Overend, G. Paraskevopoulus, Rates of OH radical reactions. 4. Reactions with methanol, ethanol, 1-propanol, and 2-propanol at 296 K, J. Phys. Chem. 82 (1978) 1329–1933.
[6] A.R. Ravishankara, D.D. Davis, Kinetic rate constants for the reaction of OH with methanol, ethanol, and tetrahydrofuran at 298 K, J. Phys. Chem. 82 (1978) 2852–2853.
[7] I.M. Campbell, D.F. McLaughlin, B.J. Handy, Rate constants for reactions of hydroxyl radicals with alcohol vapours at 292 K, Chem. Phys. Lett. 39 (1976) 362–364.
[8] E.C. Tuazon, W.P.L. Carter, R. Atkinson, J.N. Pitts Jr., The gas-phase reaction of hydrazine and ozone: a non-photolyitic source of OH radicals for measurements of relative OH radical rate constants, Int. J. Chem. Kinet. 15 (1983) 619–629.
[9] V.W. Klöpffer, R. Frank, E. Kohl, F. Haag, Quantitative erfassung der photochemischen transformationsprozesse in der troposphere, Chemiker Zeitung. 110 (1986) 57–61.
[10] B. Picquet, S. Heroux, A. Chebbi, J. Doussin, R. Durand-Jolibois, A. Monod, H. Loirat, P. Carlier, Kinetics of the reactions of OH radicals with some oxygenated volatile organic compounds under simulated atmospheric conditions, Int. J. Chem. Kinet. 30 (1998) 839–847.
[11] J. Jodkowski, M. Rayez, J. Rayez, T. Bercés, S. Dóbé, Theoretical study of the kinetics of the hydrogen abstraction from methanol. 3. Reaction of methanol with hydrogen atom, methyl, and hydroxyl radicals, J. Phys. Chem. 103 (1999) 3750–3765.
[12] R.A. Cox, A. Goldstone, Atmospheric reactivity of oxygenated motor fuel additives, in: D. Riedel (Ed.), Proceedings of the 2nd European Symposium on the "Physico-Chemical Behavior of Atmospheric Pollutants", Varese, Italy, 1982, pp. 112–119.

[13] J. Hägele, K. Lorenz, D. Rhäsa, R. Zellner, Rate constants and CH_3O product yield of the reaction OH + CH_3OH → products, Ber. Bunsenges. Phys. Chem. 87 (1983) 1023–1026.
[14] U. Meier, H.H. Grotheer, T. Just, Temperature dependence and branching ratio of the CH_3OH + OH reaction, Chem. Phys. Lett. 106 (1984) 97–101.
[15] W.P. Hess, F.P. Tully, Hydrogen-atom abstraction from methanol by OH, J. Phys. Chem. 93 (1989) 1944–1947.
[16] U. Meier, H.H. Grotheer, G. Riekert, T. Just, Study of hydroxyl reactions with methanol and ethanol by laser-induced fluorescence, Ber. Bunsenges. Phys. Chem. 89 (1985) 325–327.
[17] U. Meier, H.H. Grotheer, G. Riekert, Th. Just, Reactions in a non-uniform flow tube temperature profile: effect on the rate coefficient for the reaction C_2H_5OH + OH, Chem. Phys. Lett. 133 (1987) 162–164.
[18] W.P. Hess, F.P. Tully, Catalytic conversion of alcohols to alkenes by OH, Chem. Phys. Lett. 152 (1988) 183–189.
[19] P.G. Greenhill, B.V. O'Grady, The rate constant of the reaction of hydroxyl radicals with methanol, Aust. J. Chem. 39 (1986) 1775–1787.
[20] T.J. Wallington, M.J. Kurylo, The gas phase reactions of hydroxyl radicals with a series of aliphatic alcohols over the temperature range 240–440 K, Int. J. Chem. Kinet. 19 (1987) 1015–1023.
[21] G.L. Vaghjiani, A.R. Ravishankara, Kinetics and mechanism of OH reaction with CH_3OOH, J. Phys. Chem. 93 (1989) 1948–1959.
[22] A.J. Harrison, B.J. Cederholm, M.A. Terwilliger, Absorption of acyclic oxygen compounds in the vacuum ultraviolet. I. Alcohols, J. Chem. Phys. 30 (1959) 355–356.
[23] R. Atkinson, D.L. Baulch, R.A. Cox, R.F. Hampson Jr., J.A. Kerr, M.J. Rossi, J. Troe, Evaluated kinetic and photochemical data for atmospheric chemistry: supplement VII, organic species, J. Phys. Chem. Ref. Data. 28 (1999) 191–393.
[24] R. Atkinson, Handbook of Property Estimation Methods for Chemicals Environmental and Health Sciences CRC Press LLC, Boca Raton, FL, 2000.